Acta Med. Okayama, 2009
Vol. 63, No. 6, pp. 379–384

Acta Medica Okayama
http://escholarship.lib.okayama-u.ac.jp/amo/

Case Report

Malignant Amelanotic Melanoma of the Pleura without Primary Skin Lesion: An Autopsy Case Report

Yuichiro Ohata[a], Takayuki Haga[b], Sho Ogata[a], Kuniaki Nakanishi[a], and Toshiaki Kawai[a]*

[a]Department of Pathology and Laboratory Medicine, National Defense Medical College, Tokorozawa, Saitama 359–8513, and [b]National Higashi Saitama Hospital, Hasuda, Saitama 349–0196, Japan

Melanoma metastasizing to the lungs is common, but primary pulmonary or pleural melanoma is extremely rare. We present an autopsy case of malignant melanoma of the pleura without primary skin lesion in a 49-year-old man. A mass found in the right chest was diagnosed as spindle cell sarcoma by antemortem fine-needle aspiration cytology. At autopsy, a yellow-white tumor located primarily in the right visceral pleura (diagnosed as an amelanotic melanoma) was found to have invaded into the right lung, right parietal pleura, and right diaphragm, and to have metastasized into the left lung and visceral pleura, thyroid, and left adrenal gland. No primary site was found. The tumor cells were positive for S100 and focally positive for HMB-45, but negative for other markers. Immunohistochemical examination for S100 and HMB-45 would thus appear to be useful for the diagnosis of an amelanotic melanoma.

Key words: amelanotic melanoma, pleura, immunohistochemistry, S100, HMB-45

Malignant melanoma metastasizing to the lungs is common, but malignant melanoma has very rarely been described as a primary tumor in the lower respiratory tract. Moreover, primary pleural melanoma is so rare that the available English-language literature on pleural malignant melanoma contains only one case of such a primary tumor [1] and no case with an amelanotic melanoma of the pleura. We present here an autopsy case of malignant amelanotic melanoma of the pleura without primary skin lesion in a 49-year-old man. We discuss the histologic, immunohistochemical, and electron microscopic findings, and we present evidence favoring immunohistochemistry for S-100 and HMB-45 as a useful tool in the diagnosis of an amelanotic melanoma.

Received April 3, 2009; accepted July 27, 2009.
*Corresponding author. Phone: +81–4–2995–1505; Fax: +81–4–2996–5192
E-mail: tkawai@ndmc.ac.jp (T. Kawai)

Case Report

Some 2.5 months before he died, a 49-year-old man was admitted to the hospital for cough, right back pain, and right pleural effusion. He had a history of miliary tuberculosis at 1 month after birth. He had a 29 pack-year history of smoking. His past history was not exceptional, apart from the above.

On admission, a physical examination revealed a thumb-sized elastic, hard, subcutaneous mass in the right chest. Upon laboratory examination, WBC was increased (11.6×10^3/ml), and CRP was slightly increased (1.99 mg/ml). Among biologic tumor markers, neuron-specific enolase (NSE) was increased

(83 ng/ml; normal < 10 ng/ml). The pleural effusion was bloody, the most common leukocytes were neutrophilic ones, and the mass was diagnosed as benign by cytological examination. Chest X-ray on admission showed a large amount of right pleural effusion and a left shift of the mediastinal shadow (Fig. 1A). After drainage of the pleural effusion, chest computed tomography (CT) showed pleural thickening protruding like a nodular mass from the right thoracic wall (Fig. 1B). However, there was no abnormal finding in the left lung or in the whole-body scan (including the adrenal glands and brain). Clinically, pleural mesothelioma, cancerous pleuritis, or tuberculous pleuritis was suspected, but adenosine diaminase (ADA) (3.5 IU/l) and hyaluronic acid (83.3 ng/l) in the pleural effusion were within normal limits, and an acid-fast bacteria stain was negative. From fine needle aspiration cytology, the subcutaneous right chest mass was diagnosed as suggestive of spindle cell sarcoma (Fig. 2B). The clinician was unable to make a definite diagnosis, and the patient died about 2.5 months after admission due to respiratory failure.

Materials and Methods

Autopsy (except of the brain) was performed, and all tissues were fixed in 4% formalin, routinely processed, and stained with hematoxylin and eosin.

Immunohistochemistry was performed on de-paraffinized sections by the polymer-peroxidase method (EnVision+/HRP; Dako Cytomation, Glostrup, Denmark) using commercially available monoclonal antibodies against CAM 5.2 (Becton-Dickinson, Mountain View, CA, USA; ready-to-use), cytokeratin 5/6 (D5 & 16B4C; Cell Marque, Greenwood, AR, USA; diluted 1 : 100), cytokeratin 7 (OV-TL; 12/30; Zymed Laboratory, South San Francisco, CA, USA; ready-to-use), CK20 (Ks20.8; Nichirei, Tokyo, Japan; ready-to-use), EMA (E29; Dako; diluted 1 : 50), TTF-1 (8G7G3/1; Dako; diluted 1 : 200), α-smooth muscle actin (1A4; Dako; diluted 1: 200), desmin (D33; Nichirei; ready-to-use), CD31 (PECAM-1; Nvocastra, Newcastle Upon Tyne, UK; diluted 1 : 50), CD34 (NU-4A1; Nichirei; diluted 1 : 50), LCA (2B11; Nichirei; diluted 1 : 100), HMB45 (Dako; diluted 1 : 50), and CD117 (Nichirei; ready-to-use) as well as polyclonal antibodies against calretinin (Chemicon, Hot Springs, AR, USA; diluted 1 : 800), HHF35 (Dako; diluted 1 : 50), and S-100 (Dako; diluted 1 : 400). For CD31 expression, sections received autoclave pretreatment with 0.05 M citrate buffer, pH 6.0, for 20 min. For TTF-1 expression, sections were boiled in 0.01 mol/L Tris buffer containing 1 mM/L EDTA, pH 9.0, for 60 min.

For electron-microscopic examination, formalin-fixed specimens were first rinsed with phosphate-buffer, then transferred to 2% phosphate-buffered glutaraldehyde, postfixed in 1% osmium tetroxide, and embedded in epoxy resin. Ultrathin sections were cut and double-stained with uranyl acetate and lead citrate.

For the molecular detection of EWSR1-ATF1 or EWSR1-CREB1 (for the differential diagnosis of clear cell sarcoma), reverse transcription-polymerase

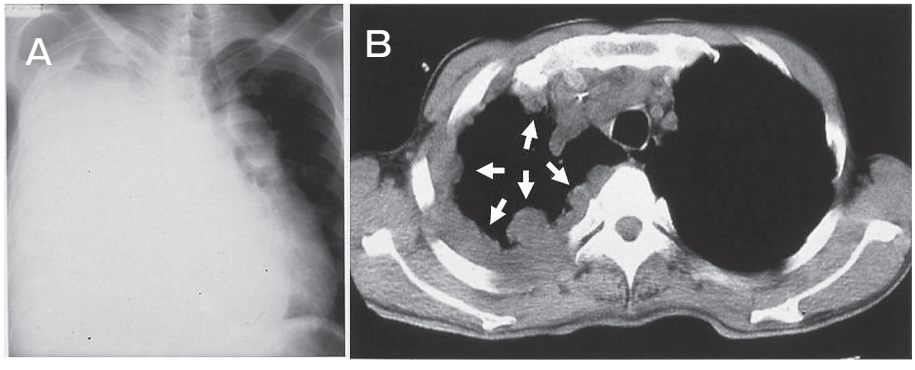

Fig. 1 Chest x-ray and computed tomography (CT). **A**, Chest x-ray on admission showed a large amount of right pleural effusion and a left shift of the mediastinal shadow; **B**, After drainage of the pleural effusion, a chest CT showed pleural thickening protruding like a nodular mass from the right thoracic wall (arrows), but no abnormal shadow in the right lung.

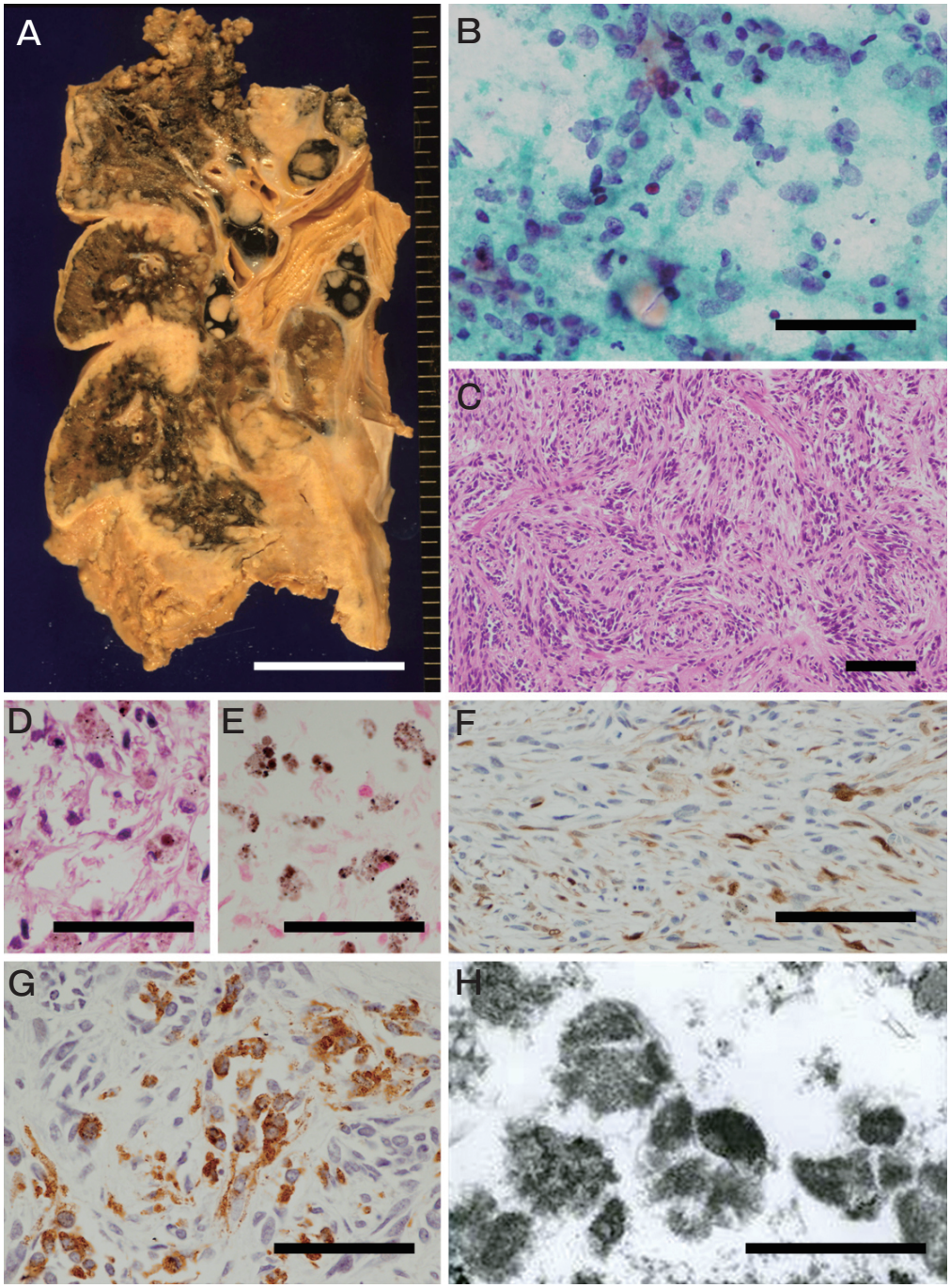

Fig. 2 Pathologic findings. **A**, Macroscopy showed a yellow-white tumor primarily located in the right visceral pleura; **B**, Fine-needle aspiration cytology obtained from the subcutaneous right chest mass revealed numerous cohesive and thick clusters of cells with a high nuclear/cytoplasmic ratio, oval nuclei, and slightly increased chromatin content; **C**, In autopsy specimens, the predominantly spindle-cell foci exhibited a fascicular growth pattern with elongated-to-ovoid pleomorphic cells possessing large hyperchromatic nuclei and vague nucleoli; **D**, Some finely granular brown pigment was present within both tumor cells and macrophages; **E**, The pigment was positive by Fontana-Masson staining; **F**, **G**, By immunohistochemistry, the tumor cells displayed a positive reaction for S100 (**F**), and were focally positive for HMB-45 (**G**, **H**) Electron microscopy revealed some vaguely lamellar or striated internal vesicles, suggestive of aberrant melanosomes. Scale bars: (**A**) 3 cm, (**B**, **C**, **D**, **E**, **F** and **G**) 100 μm, and (**H**) 1 μm.

chain reaction (RT-PCR) was performed using formalin-fixed, paraffin-embedded tumor tissues, as previously described [2]. Briefly, total RNA was extracted from the formalin-fixed, paraffin-embedded tissues using ISOGEN (Nippon Gene, Tokyo, Japan) followed by protein digestion with proteinase K (0.1 mg/ml cell lysis solution) at 55°C overnight. RT-PCR was performed using an amplification reagent kit (TaqMan EZRT-PCR kit; Applied Biosystems, Alameda, CA, USA) employing several primers. The following primers were synthesized using an automated DNA synthesizer: EWSR1-exon 7 forward, EWSR1-exon 8 forward, EWSR1-exon 9 forward, ATF1-exon 4 reverse, ATF1-exon 5 reverse, ATF1-exon 7 reverse, CREB1-exon 7 reverse, and GAPDH. Sequence information for all the PCR primers used is listed in Table 1. The reaction master mix was prepared according to the manufacturer's protocol. To perform PCR, the RT reaction was incubated at 60°C for 30 min, followed by incubation at 95°C for 5 min to deactivate AmpErase UNG. The PCR was performed using an ABI PRISM 7700 Sequence detector (Applied Biosystems) for 40 amplification cycles at 95°C for 20 sec and 60°C for 1 min. PCR products were separated by electrophoresis in a 3% agarose gel and stained with ethidium bromide.

Results

Autopsy showed that a yellow-white tumor primarily located in the right visceral pleura had invaded into the right lung tissue, and also into the right parietal pleura, diaphragm, and thoracic wall, connecting to a thumb-sized subcutaneous mass. Also evident was extensive blood vessel metastasis involving the left lung and visceral pleura, thyroid, and left adrenal gland. No primary site was found anywhere (including skin and other mucous membranes) (Fig. 2A). Histologically, the predominantly spindle-cell foci exhibited a fascicular growth pattern with elongated-to-ovoid pleomorphic cells possessing large hyperchromatic nuclei and vague nucleoli, accompanied by areas of a nuclear palisading pattern and extensive necrosis (Fig. 2C). Some nested and epithelioid foci were seen, intermingled with cartilage-like differentiation. Some finely granular brown pigment was present within both tumor cells and macrophages (Fig. 2D). Most of this pigment was positive by Fontana-Masson staining (Fig. 2E), and it was bleached by potassium permanganate, but negative by Prussian blue staining for iron.

Immunohistochemical analysis showed the tumor cells to be positive for S100 (Fig. 2F) and focally positive for HMB-45 (Fig. 2G), but negative for other markers (keratin, CAM 5.2, CK5/6, CK7, CK20, EMA, TTF-1, calretinin, α-smooth muscle actin, HHF35, desmin, CD31, CD34, CD117, and LCA). Ultrastructurally, the tumor cells were round or fusiform in shape with heterogeneous electron-dense areas. Occasionally, some showed a vaguely lamellar or striated internal structure or vesicles, suggestive of aberrant melanosomes (Fig. 2H). However, we could not rule out melanin phagocytized by melanophages. No neurosecretory granules were demonstrated. Based on the above, we diagnosed an amelanotic melanoma of the right pleura.

No PCR product was found for the type 1 fusion transcript of EWSR1-ATF1 (EWRS1-exon 8 forward and ATF1-exon 4 reverse), the type 2 fusion transcript of EWSR1-ATF1 (EWRS1-exon 7 forward and

Table 1 Primer sequences used for reverse transcription-polymerase chain reaction (RT-PCR)

Primer	Sequence
EWSR1-exon 7 forward	5'-GCC AAG CTC CAA GTC AAT ATA GC
EWSR1-exon 8 forward	5'-CAT GAG CAG AGG TGG GCG
EWSR1-exon 9 forward	5'-AGA GCG AGG TGG CTT CAA TA
ATF1-exon 4 reverse	5'-CCC CGT GTA TCT TCA GAA GAT AAG TC
ATF1-exon 5 reverse	5'-CAA CTG TAA GGC TCC ATT TGG G
ATF1-exon 7 reverse	5'-ACT CGG TTT TCC AGG CAT TT
CREB1-exon 7 reverse	5'-GTA GTA CCC GGC TGA GTG GCT G
GAPDH forward	5'-GAA GGT GAA GGT CGG AGT C
GAPDH reverse	5'-GAA GAT GGT GAT GGG ATT TC

GAPDH, glyceraldehyde-3-phosphate dehydrogenase.

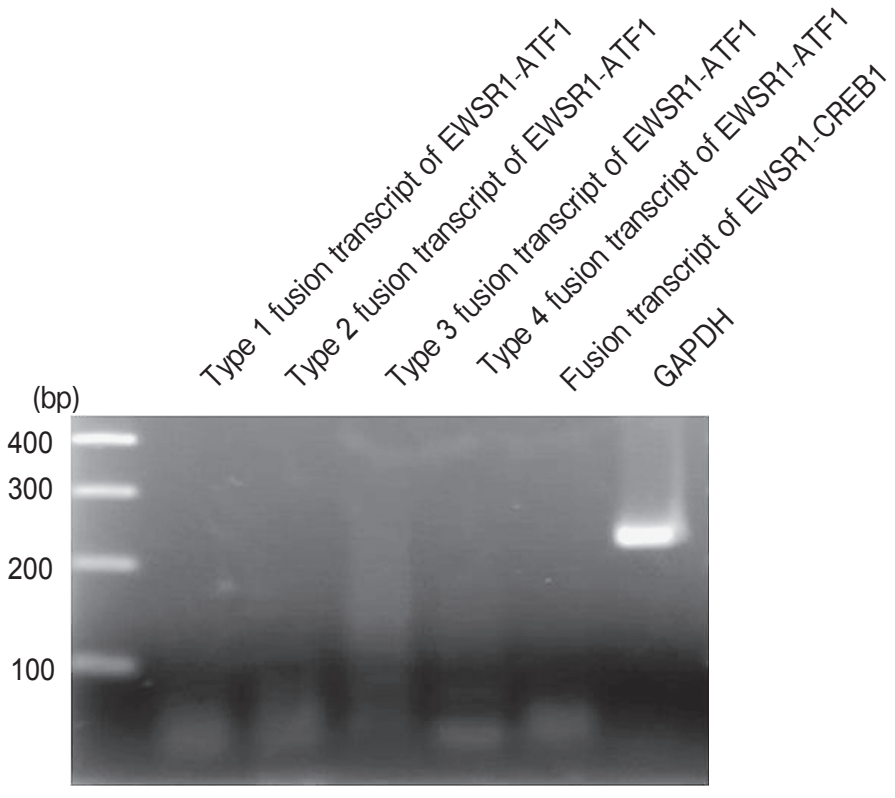

Fig. 3 PCR products for EWSR1-ATF1, EWSR1-CREB1, and GAPDH. No PCR product was found for the type 1 fusion transcript of EWSR1-ATF1 (EWRS1-exon 8 forward and ATF1-exon 4 reverse), the type 2 fusion transcript of EWSR1-ATF1 (EWRS1-exon 7 forward and ATF1-exon 5 reverse), the type 3 fusion transcript of EWSR1-ATF1 (EWRS1-exon 9 forward and ATF1-exon 5 reverse), the type 4 fusion transcript of EWSR1-ATF1 (EWRS1-exon 7 forward and ATF1-exon 7 reverse), or the fusion transcript of EWSR1-CREB1 (EWRS1-exon 7 forward and CREB1-exon 7 reverse), although GAPDH was detected.

ATF1-exon 5 reverse), the type 3 fusion transcript of EWSR1-ATF1 (EWRS1-exon 9 forward and ATF1-exon 5 reverse), the type 4 fusion transcript of EWSR1-ATF1 (EWRS1-exon 7 forward and ATF1-exon 7 reverse), or the fusion transcript of EWSR1-CREB1 (EWRS1-exon 7 forward and CREB1-exon 7 reverse), although GAPDH was detected (Fig. 3).

Discussion

Malignant melanoma has very rarely been described as a primary tumor in the pleura or lower respiratory tract. Indeed, among cases of primary pleural melanoma, only one case with malignant melanoma has been reported [1], and all 8 cases of malignant melanoma in the lower respiratory tract reported by Wilson & Moran presented as solitary, central endobronchial neoplasms [3]. In contrast, metastases of malignant melanoma to the lung or pleura are relatively common. It is therefore very important to distinguish primary from secondary melanomas. Our case is suggestive of a primary lesion of the pleura since it satisfies the following criteria for a primary melanoma of organs in which melanocytes do not exist [3, 4]: i) a solitary tumor, ii) a malignant melanoma confirmed by immunohistochemistry and/or electron microscopy, iii) no history of previous cutaneous melanoma, and iv) no demonstrable melanoma elsewhere at the time of diagnosis. However, it is known that primary cutaneous amelanotic melanoma may disappear during an advanced course [5].

It is well known that malignant altered melanocytes retain the ability to produce melanin, yet a few cases of amelanotic melanomas have been reported. Kato *et al.* [6] reported that amelanotic melanomas were present in only 2 (1.3%) of 150 cases with malignant

melanomas diagnosed in Tohoku University Hospital between 1969 and 1990. In the present case, the tumor consisted, histologically, of predominantly spindle-cell foci with a fascicular growth pattern accompanied by areas of a nuclear palisading pattern. In our immunohistochemical examination, tumor cells were negative for epithelial (keratin and EMA) and myogenic (desmin and α-smooth muscle actin) markers. However, in some tumor cells we found finely granular brown pigments that exhibited a positive reaction to Fontana-Masson staining. Furthermore, tumor cells displayed a positive immunoreaction for melanocytic markers (S100 and HMB-45). We therefore diagnosed an amelanotic melanoma of the right pleura. To judge from the above findings, an immunohistochemical examination for S-100 and HMB-45, together with Fontana-Masson staining, is a useful tool for the diagnosis of an amelanotic melanoma.

Two important differential diagnoses should be mentioned in the present case: one is pleural mesothelioma, the other is clear cell sarcoma. The gross appearance in the present case showed a mass within and around the right visceral pleura, similar to the masses seen in pleural mesothelioma (Fig. 2A). However, no staining was found for imunohistochemical markers such as keratin, CAM 5.2, CK5/6, CK7, CK20, EMA, or calretinin. The latter tumor, clear cell sarcoma, is a malignant soft tissue tumor with melanocytic differentiation. Even if such a tumor is not detected, CD117 immunoreactivity, recurrent chromosomal translocation t (12 ; 22) (q13 ; q12), or a resultant fusion of the EWSR1 gene on 22q12 and the ATF1 gene on 12q13 is specifically detected in most cases of clear cell sarcoma [2]. Furthermore, another variant fusion gene, EWSR1-CREB1, has been found in a patient with clear cell sarcoma [2]. Therefore, fusion gene transcripts of either EWSR1-ATF1 or EWSR1-CREB1 are detected. In our case, however, no CD117 immunoreactivity or EWSR1-ATF1 or EWSR1-CREB1 fusion gene transcripts were detected.

The histogenesis of malignant melanoma of the pleura is unclear. One explanation might be that cutaneous nevus cells enter dermal lymphatic vessels, and then travel via the lymphatic system to the pleura. In fact, Biddle *et al.* reported that nevus-cell aggregates originating from the skin can reach the lymph nodes via the lymphatic system [7]. If nevus cells can migrate to the pleura in a similar way, they could be the source of malignant melanoma. However, we know of no report of nevus-cell migration to the pleura, so this idea must remain speculative.

References

1. Smith S and Opipari MI: Primary pleural melanoma. A first reported case and literature review. J Thorac Cardiovasc Surg (1978) 75: 827–831.
2. Hisaoka M, Ishida T, Kuo TT, Matsuyama A, Imamura T, Nishida K, Kuroda H, Inayama Y, Oshiro H, Kobayashi H, Nakajima T, Fukuda T, Ae K and Hashimoto H: Clear cell sarcoma of soft tissue: a clinicopathologic, immunohistochemical, and molecular analysis of 33 cases. Am J Surg Pathol (2008) 32: 452–460.
3. Wilson RW and Moran CA: Primary melanoma of the lung: a clinicopathologic and immunohistochemical study of eight cases. Am J Surg Pathol (1997) 21: 1196–1202.
4. Jennings TA, Axiotis CA, Kress Y and Carter D: Primary malignant melanoma of the lower respiratory tract. Report of a case and literature review. Am J Clin Pathol (1990) 94: 649–655.
5. Jonk A, Kroon BB, Rümke P, Mooi WJ, Hart AA and van Dongen JA: Lymph node metastasis from melanoma with an unknown primary site. Br J Surg (1990) 77: 665–668.
6. Kato T, Suetake T, Sugiyama Y, Tanita Y, Kumasaka K, Takematsu H, Tomita Y and Tagami H: Improvement in survival rate of patients with acral melanoma observed in the past 22 years in Sendai, Japan. Clin Exp Dermatol (1993) 18: 107–110.
7. Biddle DA, Evans HL, Kemp BL, El-Naggar AK, Harvell JD, White WL, Iskandar SS and Prieto VG: Intraparenchymal nevus cell aggregates in lymph nodes: a possible diagnostic pitfall with malignant melanoma and carcinoma. Am J Surg Pathol (2003) 27: 673–681.